IMPACT PROPERTIES OF GLASS FIBER COMPOSITES WITH RESPECT TO SURFACE TREATMENT AND FIBER VOLUME FRACTION

S. S. Cheon[1] and D. G. Lee[2]

[1] *Automotive component div. Daesung Group, 155-2, Kwanhoon-dong, Chongro-gu, Seoul, 110-300, Korea*
[2] *Mechanical Design Laboratory with Advanced Materials, ME3221, Department of Mechanical Engineering, Korea Advanced Institute of Science and Technology 373-1, Gusong-dong, Yusong-gu, Taejon, 305-701, Korea*

SUMMARY: The impact energy absorption characteristics of glass epoxy composites and glass polyester composites with respect to fiber volume fraction were investigated by the instrumented Charpy impact test method. Also, the glass polyester composites both with and without silane treatment were tested. The interlaminar shear properties were measured by the short beam shear test to investigate the correlation between the interlaminar shear properties and the impact energy absorption characteristics. Additionally, the glass epoxy hybrid composites embedded with glass fibers without silane treatment were tested. From the tests, the optimum fiber volume fraction for impact energy absorption was obtained and the progressive impact fracture model was proposed to predict the impact absorption characteristics of composites.

KEYWORDS: impact energy absorption, interlaminar properties, silane coupling treatment, progressive impact fracture model

INTRODUCTION

Fiber reinforced composites have high specific stiffness (stiffness/density), specific strength (strength/density), and damping characteristics. Due to these beneficial properties, they have been used for structural materials of aircraft and space vehicles. As low cost manufacturing technologies and mass production methods for composite structures have been developed, the applications of composite materials to leisure sport goods and auto bodies are being increased nowadays [1]. Recent studies show that the successful applications of composites to mechanical elements or structures [2-6] have been accomplished, and the research reports from the United States and Canada [7] have predicted that almost all structures of automobiles will be replaced with composites until the 21st centuries. However, composite structures are vulnerable to impact, which limits the applicability of composites to dynamic structures. The impact absorption capability of composite materials is dependent upon the interfacial strength between fiber and matrix. Also the mechanical behavior including impact behavior of

composites is much dependent on the fiber volume fraction. Many researchers have widely studied about these features of composites. Bader et al. [8] investigated the impact behavior of carbon fiber epoxy composite materials using the Charpy impact test of V-notched specimens. Yeung et al. [9] treated the surface of the glass fiber with silane coupling agent and investigated the effect of interface strength on the impact properties of glass epoxy and glass polyester composites. Sun et al. [10] modeled the highly nonlinear behavior of the laminate in the penetration process of thick laminates during a high velocity impact proposing a simple ring element which was based on the Minddlin beam theory. Harding et al. [11] obtained the dynamic stress-strain relationships of unidirectional carbon fiber epoxy and fabric glass fiber epoxy composites using the modified tensile split Hopkinson bar tester. Caprino [12] predicted the residual strength of impacted carbon fiber reinforced composites. Choi et al [13] proposed a novel approach for damage mechanisms due to low velocity impact. Kim et al [14] investigated the impact resistance of the honeycomb inserted composite sandwich laminate. Sirkis et al. [15] examined the micro crack distribution in the vicinity of optical fiber embedded graphite epoxy laminate panels subjected to low velocity impact. Rashkovan et al. [16] investigated the fiber surface treatment effect on the adhesion of epoxy or polyamide matrices by the single fiber composite test. In this study, the impact energy absorption characteristics of glass epoxy composites and glass polyester composites were investigated with respect to fiber volume fraction by the instrumented Charpy impact test method. Also, the effects of silane treatment on the glass polyester composites were tested. Additionally, the composite specimens which contained both the fibers with and without silane treatment were tested. The interlaminar shear properties were measured by the short beam shear test to investigate the correlation between the interlaminar shear properties and the impact energy absorption characteristics. From the tests, the optimum fiber volume fraction for impact energy absorption was obtained and the progressive impact fracture model was proposed to predict the impact absorption characteristics of composites.

SHORT BEAM SHEAR TEST AND INSTRUMENTED CHARPY IMPACT TEST

In order to investigate the effect of the surface treatment and interface strength on the impact absorption characteristics of composite materials, several types of composite specimens were prepared: glass epoxy composite, glass polyester composites with and without silane treatment of glass fiber and the glass epoxy hybrid composites embedded with glass fibers without silane treatment. For the glass epoxy composite specimens, 40 ply glass epoxy prepregs (UGN 150, SK Chemicals, Suwon, Korea) were stacked. The resin content of the specimens was controlled by the amount of resin bleeder used during autoclave vacuum bag degassing molding process. During this process, the composite specimens underwent 80 dwelling about 30 minutes for consolidation, and 120 dwelling two and half hours for main curing. Also, 0.6 MPa pressure was applied outside the vacuum bag. The fiber volume fraction of the glass epoxy composite laminates in this work ranged from 54.2 to 70.7%. The glass polyester composite specimens were manufactured by winding the resin wetted glass fiber roving on a mandrel. The surface of glass fibers was treated with silane coupling agent and the orthophthalic polyester resin (Polycoat FH102HS, Aekyung Chemical Co., Taejon, Korea) was used for the glass fiber polyester laminates. Also, the laminates were manufactured using the same polyester resin and glass fiber without silane treatment to make the interface between the fiber and the matrix weak. The fiber volume fraction of the composite laminates was controlled by the amount of resin bleeder used. The glass polyester composite specimens underwent 80 dwelling about 15 minutes for main curing under 0.6 MPa pressure outside the vacuum bag. The fiber volume fraction of the glass polyester composite laminates in this work ranged from

53.4 to 75.7% and that of glass fiber without silane treatment polyester composites from 51.8 to 69.7%. For the glass epoxy composite specimens with weak interface, the glass fiber without silane treatment was embedded in the middle layer of the glass epoxy prepregs. The volume fraction of the glass fibers without silane treatment from 1.8 to 9% relative to the total specimen volume was used. The maximum interlaminar shear stress of a rectangular beam of width *w* and thickness *h* subjected to a load of P_B is expressed as follows.

$$t_Y = \frac{3P_B}{4wh} \tag{1}$$

Table 1 shows the mechanical properties of the two composite materials when the fiber volume fraction was 54 %.

Table 1. Mechanical properties of the composite specimens.

(fiber volume fraction: 54%)

	Glass epoxy	Glass polyester
Longitudinal tensile modulus (GPa)	43	40
Longitudinal tensile strength (MPa)	1021	611
Major Poisson's ratio	0.28	0.25

The fiber volume fractions of the composites were measured both by the matrix digestion and by the sintering methods. It was found that the two methods gave almost the same fiber volume fraction for each composite specimen. The test specimens were made by cutting the plate in the fiber direction with a diamond wheel cutter. The dimensions for the short beam shear test and the instrumented Charpy impact test were 5×28×4 mm and 10×55×4 (width × length × thickness, mm), respectively. The short beam shear tests were performed using Instron 4206 static material tester. The ratio of span to thickness was set to be 5, and the nose radii of the loading cylinder and the supporting fixtures were 3.15mm and 1.6mm, respectively as recommended by ASTM D2344-84. The crosshead speed was set to be 0.3 mm/min.

For the glass epoxy composite, the interlaminar shear strength increased slightly at first as the fiber volume fraction increased as shown in Fig. 1 (a). However, it decreased after the fiber volume fraction exceeded 60%. For the glass polyester composite, on the contrary, the interlaminar shear strength decreased at first as the fiber volume fraction increased, then slightly increased when the fiber volume fraction exceeded 70% as shown in Fig. 1 (b). For the not-silane-treated glass polyester composite in Fig. 1 (c), the interlaminar shear strength was very low and its failure mode was ductile during yielding with the deep indentation and the compressive fiber buckling. For the glass epoxy composite embedded with the not-silane-treated glass fibers, the interlaminar shear strength was slightly decreased as shown in Fig. 1 (d) because of the weak bonding forces between the embedded fiber and the matrix. Also, the first failure occurred at the interface between the not-silane-treated glass fiber and the glass epoxy composite. From the short beam shear test, it was found that the higher the fiber volume fraction was, the more the ply interfaces for both the glass epoxy and the glass polyester composites were delaminated irrespective of silane treatment. As the fiber volume fraction was increased, the delamination failure mode changed from the propagation dominant to the initiation dominant.

The impact energy absorption tests were performed using the instrumented Charpy impact tester (SI-1B type, Satec Systems, U.S.A). The signals from the sensors and the load cell of the impact tester were transferred into a personal computer through the Dynatup GRC 830-I program. The impact characteristics of fiber reinforced composite beams may be overestimated

when the span to thickness ratio is smaller than the critical value which is dependent on fiber and resin types. Since the critical value exists in the range of 4-6 for most composite beams [8], in this work, the span length was set to be 40 mm, which yielded the value of span to thickness ratio of 9-13. The notch free Charpy specimens were prepared because the notch effect was known to be negligible for composite specimens [8]. The impact speed was fixed to be 5.21 m/s and the employed hammer mass was 12.07 kg. The force transducer was mounted on the tup section of 3 mm nose radius. The load and energy absorption histories versus time were measured using a personal computer. The total impact energy absorption E was obtained by integrating the fracture initiation and propagation energy components as follows.

$$E = \int_0^{t_f} P \cdot v dt \tag{2}$$

Where P is the dynamic load acting on the specimen, v the impact speed, t_f the time beyond which the dynamic load becomes zero. The load-time diagrams during impact tests can be divided into the fracture initiation and the fracture propagation stage. During the fracture initiation stage, the elastic energy is accumulated in the specimen until the occurrence of first failure.

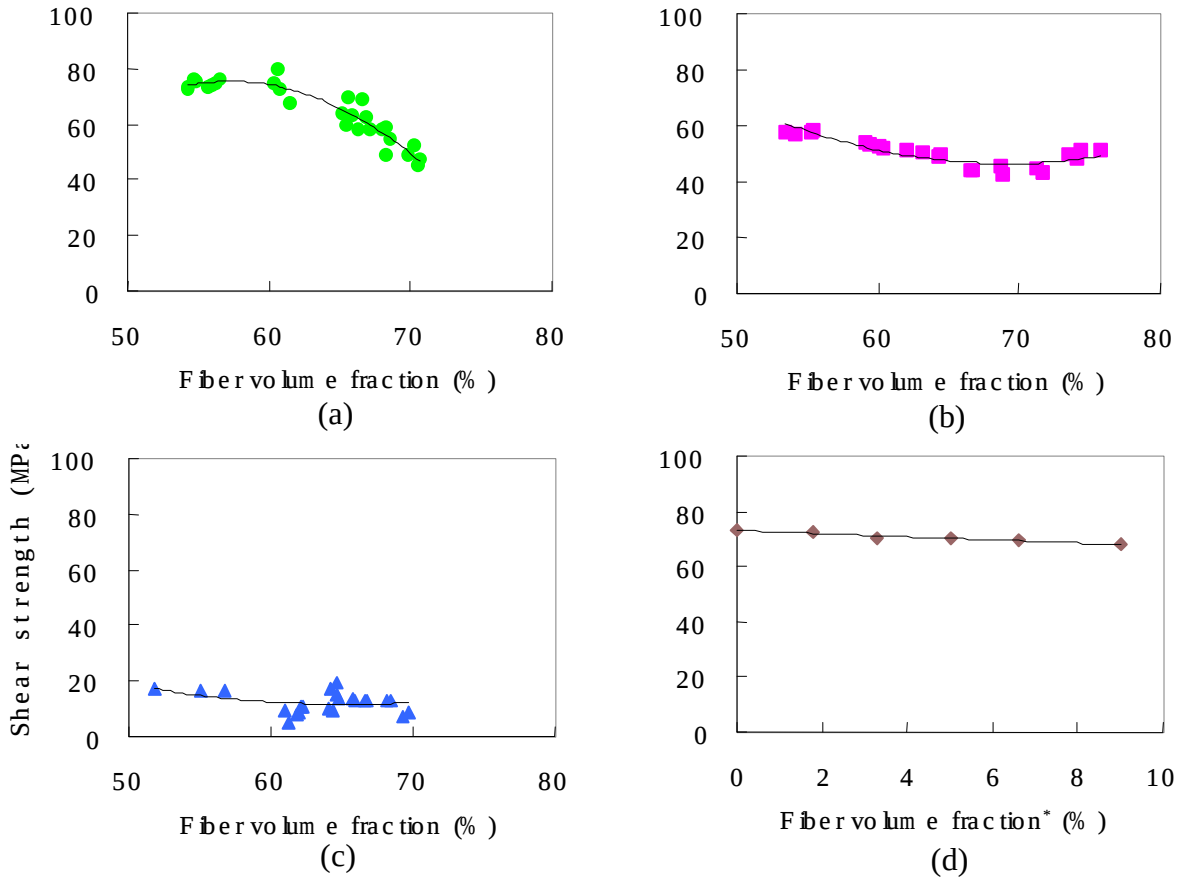

*Fig. 1: Static interlaminar shear strengths of composites versus fiber volume fraction: (a) glass epoxy composite, (b) silane-treated glass fiber polyester composite, (c) not-silane-treated glass fiber polyester composite, (d) glass fiber epoxy composites embedded with not-silane-treated glass fibers, * volume fraction of the additionally embedded not-silane-treated glass fibers.*

Fig. 2 shows the impact energy absorption versus fiber volume fraction for each composite specimen. From the impact tests of the glass epoxy composites, it was found that the delamination started at the impacted site and propagated perpendicularly to the loading direction. As the fiber volume fraction was increased, the energy absorption due to the fiber breakage and fiber pull-out was increased until the fiber volume fraction of 65%, then it was decreased because the interlaminar crack was easily propagated through the composite specimens without fiber breakage and fiber pull-out due to the decrease of the interlaminar shear strength. Consequently the impact energy absorption capability was decreased as the fiber volume fraction was increased beyond 65 %.

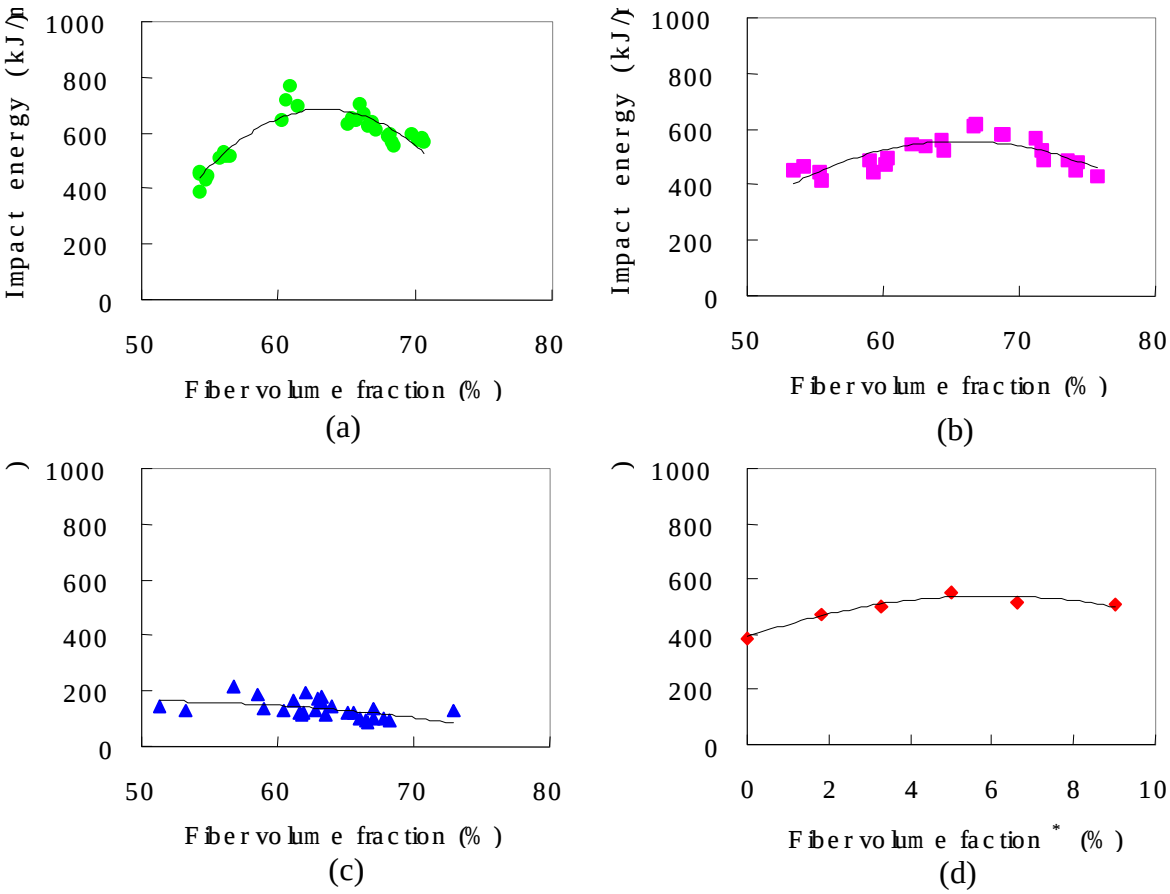

*Fig. 2: Impact energy absorption per unit area versus fiber volume fraction: (a) glass epoxy composite, (b) silane-treated glass fiber polyester composite, (c) not-silane-treated glass fiber polyester composite, (d) glass fiber epoxy composites embedded with not-silane-treated glass fibers, * volume fraction of the additionally embedded not-silane-treated glass fibers.*

From the impact tests of the silane-treated glass polyester composites, it was found that the modes of delamination failure were similar to those of glass epoxy composites. However, for the glass polyester composites, it was found that the fiber breakage and fiber pull-out occurred in the whole range of fiber volume fraction tested, which divided the specimens into two or more parts. When the fiber volume fraction of these composites was lower than 60%, the specimen was divided into two parts by interlaminar delamination crack. Therefore, the fiber breakage and pull-out failure were not extensive. As the fiber volume fraction was increased, the specimens were also failed by the delamination, however, with more extensive fiber breakage and pull-out failure. As the fiber volume fraction approached 70%, the interlaminar delamination cracks were created at many interfaces and easily propagated through the

specimen due to lack of resin between the fibers. Consequently, the impact energy absorption capability decreased when the fiber volume fractions were high; the impact absorption capabilities of the glass fiber epoxy specimens and the silane-treated glass fiber polyester specimens were decreased beyond the 65% and 70% of fiber volume fraction, respectively. From these results, it was concluded that there existed an optimum interlaminar shear strength, which gave the maximum energy absorption due to fiber breakage, fiber pull-out and delamination.

Although, the impact energy absorption capability of the not-silane-treated glass fiber polyester composite specimens was decreased slightly as the fiber volume fraction increased, it was concluded that there was no prominent tendency of impact energy absorption characteristics of this type of composite specimens. Also, it was found that the fiber breakage and fiber pull-out failure of these specimens did not occur in the whole range of fiber volume fraction tested and the impact energy absorption capability was too low for practical application compared to other types of composite specimens. When the not-silane-treated glass fiber of 5 % volume fraction was embedded in the middle layer of the glass epoxy composite, the impact energy absorption was increased 40 % compared to that of the glass epoxy composite without embedding.

PROGRESSIVE IMPACT FRACTURE MODEL

In order to predict the dynamic external load and the energy absorption during the Charpy impact test, the progressive impact fracture model was proposed in this study. The basic scheme of this method is to eliminate the fractured part of the specimen at each loading stage. A simple differential equation could be derived from the Charpy impact test.

$$m\ddot{y} + ky = 0 \tag{3}$$

Where m is the impactor mass. For the simply supported center loading, equivalent spring constant k can be obtained from the mechanics of materials method.

$$k = \frac{48EI}{L^3} \tag{4}$$

Where, E, I and L represent the Young's modulus, the second moment of inertia and the span length, respectively. E can be calculated using the rule of mixture. The solution of the equation (3) is as follows.

$$y = v\sqrt{\frac{mL^3}{4Ewh^3}}\,sin\left(\sqrt{\frac{4Ewh^3}{mL^3}}t\right) \tag{5}$$

Since the glass epoxy composite has larger tensile strength (1GPa) than compressive one (600MPa), the glass fiber composite specimens would undergo the fracture of the upper part first. If the composite specimen were failed by the interlaminar stress, the specimen would split into two pieces and then the outer parts of the split specimens would fail by the tensile or compressive stress.

The times t_t and t_c required for which the bending stress in the composite specimen reached the tensile strength and compressive strength, respectively and t_s required for the interlaminar

shear stress reached the shear strength, were calculated as follows.

$$t_t = \sqrt{\frac{mL^3}{4Ewh^3}}\sin^{-1}\left(\frac{\sigma_t}{3\nu}\sqrt{\frac{Lhw}{mE}}\right) \tag{6-a}$$

$$t_c = \sqrt{\frac{mL^3}{4Ewh^3}}\sin^{-1}\left(\frac{\sigma_c}{3\nu}\sqrt{\frac{Lhw}{mE}}\right) \tag{6-b}$$

$$t_s = \sqrt{\frac{mL^3}{4Ewh^3}}\sin^{-1}\left(\frac{2\tau_d}{3\nu}\sqrt{\frac{L^3w}{mEh}}\right) \tag{6-c}$$

Where, σ_t, σ_c and τ_d represent the tensile, compressive and interlaminar shear strengths of the glass epoxy composite, respectively. Equations (6-a) and (6-b) were derived from the bending stress relation, and Equation (6-c) was derived from Equation (1). Since the tensile and compressive moduli of the glass fiber composite are different, but they are within around 10% difference [17], in this study they were assumed to be equal. The next step is to choose the minimum time among t_t, t_c and t_s. If t_t were selected, then the composite specimens would undergo the fracture of the base part. If t_c were selected, then the fracture of the upper part of the composite specimen would occur. If t_s were selected, then it would go through the interlaminar fracture. In this study, t_c was the smallest among them in all cases. During calculation, it was assumed that the actual compressive fracture of the composite specimens occurred at 1.1 t_c rather than at t_c to make the eliminated part by fracture finite. Then, the composite specimen thickness $\tilde{h}$ after eliminating the fractured part by compression from the original thickness h was calculated as follows.

$$\tilde{h} = \frac{h}{2} + \frac{\sigma_c}{6\nu}\sqrt{\frac{Lwh^3}{mE}}\csc\left(1.1t_c\sqrt{\frac{4Ewh^3}{mL^3}}\right) \tag{7}$$

Accordingly, the second moment of inertia of the composite specimen and the velocity of the impactor should be updated in each iteration process as the fractured part of the composite specimen was eliminated.

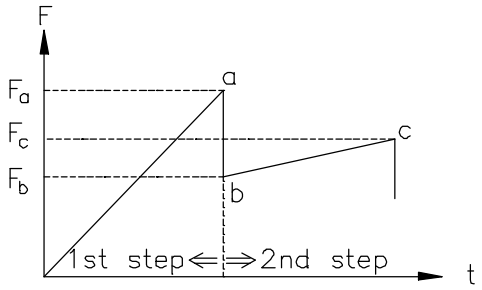

Fig. 3: Schematic force F versus time t diagram of the progressive impact fracture model for the composite specimen.

To start the next step iteration, it is essential to determine the beginning force F_b as shown in

Fig. 3. Since the displacement of the impactor at the end of the first step is equal to that of the start of the second step, the following relationship holds.

$$F_b = \frac{k_b}{k_a} F_a \tag{8}$$

Where k_a and k_b are the stiffnesses of the composite specimen during the 1st step and the 2nd step, respectively. As explained above, the iterative procedure would result in the dynamic load and the energy absorption versus time graphs. During each step of the iteration, the displacement of the impactor was calculated and compared to the critical displacement of the impactor which was defined by the Pythagorean theorem as follows.

$$\mathrm{d}_c = \sqrt{\left(\frac{L_s}{2}\right)^2 - \left(\frac{L}{2}\right)^2} \tag{9}$$

Where L_s and L is the specimen length and the span length, respectively. If the displacement of the impactor were larger than this critical value, the hybrid composite specimen would no longer support external loads, but slip through the jig of the Charpy impact tester. At that time, the iteration would be terminated. Fig. 4 shows the comparison results between the Charpy impact test and the progressive impact fracture model.

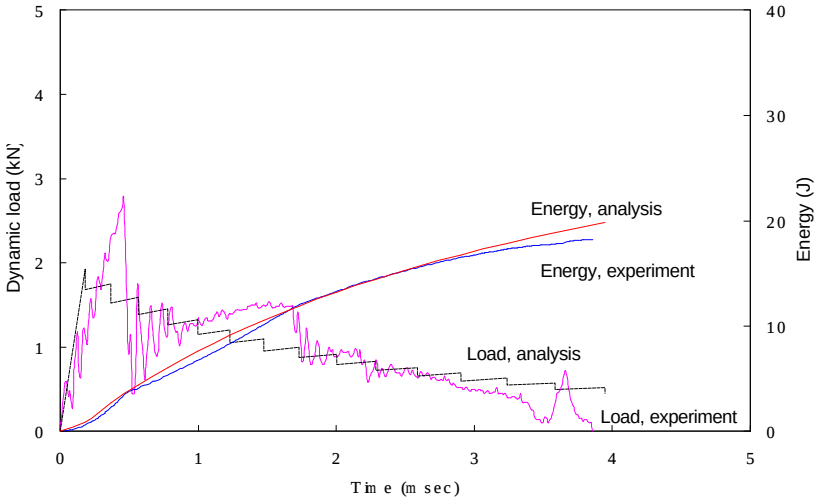

Fig. 4: Analytical and experimental results of the external load and energy absorption.

In Fig. 4, neglecting the Herzian contact brought about the slight discrepancy of the initial slope between analysis and experiment curves of the dynamic load. Also, the peak load value of the analysis was smaller than that of the experiment. This may come from the fact that the high strain rate would enhance the tensile or compressive strength of the glass epoxy composites [11].

CONCLUSIONS

In this work, the impact energy absorption characteristics of the glass epoxy composites and the glass polyester composites were investigated by the instrumented Charpy impact test method with respect to the fiber volume fraction.

For the glass epoxy composites, the maximum impact energy absorption as well as the maximum shear strength were obtained at the fiber volume fraction of around 60% with the dominant failure modes of fiber breakage and fiber pull-out. For the silane-treated glass fiber polyester composites, the maximum impact energy absorption was obtained when the fiber volume fraction was 65-70% with the fiber breakage, fiber pull-out and extensive delamination. For the silane-treated glass fiber polyester composites, the impact energy absorption characteristics were slightly decreased as the fiber volume fraction was increased from 52% to 70%. The glass epoxy composites absorbed the highest energy, while the not-silane-treated glass polyester composites absorbed the lowest one. It was found that the silane-treated fiber composites showed brittle behavior and were more sensitive to the rate of loading. The failure mode of unidirectional continuous fiber composites was changed from the fiber breakage and fiber pull-out modes to the delamination dominant mode as the fiber volume fraction was increased. When the unidirectional glass fiber epoxy composites were embedded with the 5% not-silane-treated glass fibers, the impact energy absorption capability was 40 % higher than that of the pure glass fiber epoxy composite. The progressive impact fracture model that was proposed to predict the dynamic load and the energy absorption during the impact of the composites showed relatively good agreement with the experimentally obtained impact energy absorption characteristics.

ACKNOWLEDGMENTS

This work was supported by **KOSEF** (Korea Science and Engineering Foundation) under Grant No. 98-02-00-01-01-5. Their support is gratefully acknowledged. Also, the authors were grateful to Kim Joo Hak, senior researcher in **KAERI** (Korea Atomic Energy Research Institute) for helping Charpy impact test, Hyundai fiber glass co. for granting the glass fiber without silane treatment and Aekyung Chemical Co. Ltd. for granting the polyester resin.

REFERENCES

1. Mallick, P.K., *Fiber Reinforced Composites,* Marcel Dekker Inc., New York, 1988.

2. Lee, D.G., Sin, H.C. and Suh, N.P., "Manufacturing of a Graphite Epoxy Composite Spindle for a Machine Tool," *Annals of CIRP*, Vol. 34, 1985, pp. 365-369.

3. Lee, D.G., Jeong, K.S., Kim, K.S. and Kwak, Y.K., "Development of the Anthropomorphic Robot with Carbon Fiber Epoxy Composite Materials," *Composite Structures*, Vol. 25, 1993, pp. 313-324.

4. Cho, D.H. and Lee, D.G., "Manufacturing of Cocured Hybrid Aluminum Composite Shafts with Preload to Reduce Residual Thermal Stresses," *Journal of Composite Materials*, Vol. 32, 1998, pp. 1221-1241.

5. Choi, J.K. and Lee, D.G., "Manufacturing of a Carbon Fiber-epoxy Composite Spindle-bearing System for a Machine Tool," *Composite Structures*, Vol. 37, 1997, pp. 241-251.

6. Cheon, S.S., Choi, J.H. and Lee, D.G., "Development of the Composite Bumper Beam for Passenger Cars," *Composite Structures*, Vol. 32, 1995, pp. 491-499.

7. 1992. *Automotive Plastics Report 92*: Market Search Inc., Sec 1., p. 17.

8. Bader, M.G. and Ellis, R.M., "The Effect of Notches and Specimen Geometry on the Pendulum Impact Strength of Uni-axial CFRP," *Composites*, Vol. 6, 1974, pp. 253-258.

9. Yeung, P. and Broutman, L.J., "The Effect of Glass-Resin Interface Strength on the Impact Strength of Fiber Reinforced Plastics," *Polymer Engineering and Science*, Vol. 18, 1978, pp. 62-72.

10. Sun, C. T. and Potti, S. V., A Simple Model to Predict Residual Velocities of thick Composite Laminates Subjected to High Velocity Impact. *International Journal of Impact Engineering*, Vol. 18, 1996, pp. 339-353.

11. Harding, J. and Welsh, L.M., "A Tensile Testing Technique for Fibre-Reinforced Composites at Impact Rates of Strain," *Journal of Materials Science*, Vol. 18, 1983, pp. 1810-1826.

12. Caprino, G., "Residual Strength Prediction of Impacted CFRP Laminates," *Journal of Composite Materials*, Vol. 18, 1984, pp. 508-518.

13. Choi, H.Y., Wu, H.Y. and Chang, F.K., "A New Approach toward Understanding Damage Mechanisms and Mechanics of Lminated Composites Due to Low-velocity Impact: Part II-Analysis," *Journal of Composite Materials*, Vol. 25, 1991, pp. 1012-1038.

14. Kim, C.G. and Jun, E.J., "Impact Resistance of Composite Laminated Sandwich Plates," *Journal of Composite Materials*, Vol. 26, 1991, pp. 2247-2261.

15. Sirkis, J.S. and Chang, C.C., "Low velocity impact of Optical Fiber Embedded Laminated Graphite/Epoxy Panels," *Journal of Composite Materials*, Vol. 28, 1994, pp. 1532-1552.

16. Rashkovan, I.A. and Korabel'nikov, Y.G., "The Effect of fiber Surface Treatment on Its Strength and Adhesion to the Matrix," *Composites Science and Technology*, Vol. 57, 1997, pp. 1017-1022.

17. Agarwal, B.D. and Broutman, L.J., *Analysis and Performance of Fiber Composites*, John Wiley & Sons, Inc. 1990, p.103.